

# Myocardial Work, an Echocardiographic Measure of Post Myocardial Infarct Scar on Contrast-Enhanced Cardiac Magnetic Resonance

Mohammed El Mahdiui, MD<sup>a</sup>, Pieter van der Bijl, MB, ChB, MMed<sup>a</sup>, Rachid Abou, MD<sup>a</sup>, Rodolfo de Paula Lustosa, MD<sup>a</sup>, Rob van der Geest, PhD<sup>b</sup>, Nina Ajmone Marsan, MDPhD<sup>a</sup>, Victoria Delgado, MD, PhD<sup>a</sup>, and Jeroen J. Bax, MD, PhD<sup>a,c,\*</sup>

**This study investigates the relation of non-invasive myocardial work and myocardial viability following ST-segment elevation myocardial infarction (STEMI) assessed on late gadolinium contrast enhanced cardiac magnetic resonance (LGE CMR) and characterizes the remote zone using non-invasive myocardial work parameters. STEMI patients who underwent primary percutaneous coronary intervention (PCI) were included. Several non-invasive myocardial work parameters were derived from speckle tracking strain echocardiography and sphygmomanometric blood pressure, e.g.: myocardial work index (MWI), constructive work (CW), wasted work (WW) and myocardial work efficiency (MWE). LGE was quantified to determine infarct transmural and scar burden. The core zone was defined as the segment with the largest extent of transmural LGE and the remote zone as the diametrically opposed segment without LGE. A total of 53 patients (89% male, mean age  $58 \pm 9$  years) and 689 segments were analyzed. The mean scar burden was  $14 \pm 7\%$  of the total LV mass, and 76 segments (11%) demonstrated transmural hyperenhancement, 280 (41%) non-transmural hyperenhancement and 333 (48%) no LGE. An inverse relation was observed between segmental MWI, CW and MWE and infarct transmural ( $p < 0.05$ ). MWI, CW and MWE were significantly lower in the core zone compared to the remote zone ( $p < 0.05$ ). In conclusion, non-invasive myocardial work parameters may serve as potential markers of segmental myocardial viability in post-STEMI patients who underwent primary PCI. Non-invasive myocardial work can also be utilized to characterize the remote zone, which is an emerging prognostic marker as well as a therapeutic target. © 2021 The Authors. Published by Elsevier Inc. This is an open access article under the CC BY-NC-ND license (<http://creativecommons.org/licenses/by-nc-nd/4.0/>) (Am J Cardiol 2021;00:1–9)**

Accurate quantification of the extent and transmural of myocardial infarct in patients following an ST-segment elevation myocardial infarction (STEMI) is essential in the identification of viable myocardial regions that could benefit from revascularization.<sup>1</sup> In addition, the remote zone, i.e. the non-infarcted myocardium remote from the infarct core, is an emerging region of interest in STEMI, with the potential to be used as a therapeutic target.<sup>2-4</sup> Late gadolinium contrast enhanced cardiac magnetic resonance (LGE CMR) is the gold standard for the quantification of the extent of transmural scar<sup>5</sup> with high reproducibility<sup>6</sup> and a robust association with prognosis.<sup>5,7</sup> The use of CMR is limited by availability, time and cost. Recently, non-invasive myocardial work has been proposed as a parameter for assessing left ventricular (LV) systolic function.<sup>8,9</sup> The ability of non-invasive myocardial work indices to characterize post-

infarct scar and myocardial function has not been investigated. The aims of the current study were to explore the relation of non-invasive myocardial work indices to transmural of post-infarct scar on LGE CMR, and to compare myocardial work indices between infarct core and remote zone.

## Methods

Patients admitted with an acute STEMI who underwent primary percutaneous coronary intervention (PCI) between 2004 and 2017 at the Leiden University Medical Center (LUMC) were evaluated.<sup>10</sup> For this study, only patients with feasible non-invasive myocardial work analysis by 2-dimensional speckle-tracking strain echocardiography and with LGE CMR data were selected for analysis. Patients with prior myocardial infarction, coronary artery bypass grafting, LGE CMR performed within 30 days of index myocardial infarction, non-feasible 2-dimensional speckle-tracking strain echocardiography, moderate to severe valve disease or missing blood pressure measurements were excluded (Figure 1). Patients were treated according to prevailing guidelines from the European Society of Cardiology, as described previously.<sup>10</sup> The culprit vessel was identified during invasive coronary angiography and

<sup>a</sup>Department of Cardiology, Leiden University Medical Center, Leiden, The Netherlands; <sup>b</sup>Department of Radiology, Leiden University Medical Center, Leiden, The Netherlands; and <sup>c</sup>Heart Center, University of Turku and Turku University Hospital, Turku, Finland. Manuscript received February 1, 2021; revised manuscript received and accepted April 6, 2021.

See page 8 for disclosure information.

\*Corresponding author: Tel.: (31) 71 526 2020; fax: (31) 71 526 6809.

E-mail address: [J.J.Bax@lumc.nl](mailto:J.J.Bax@lumc.nl) (J.J. Bax).

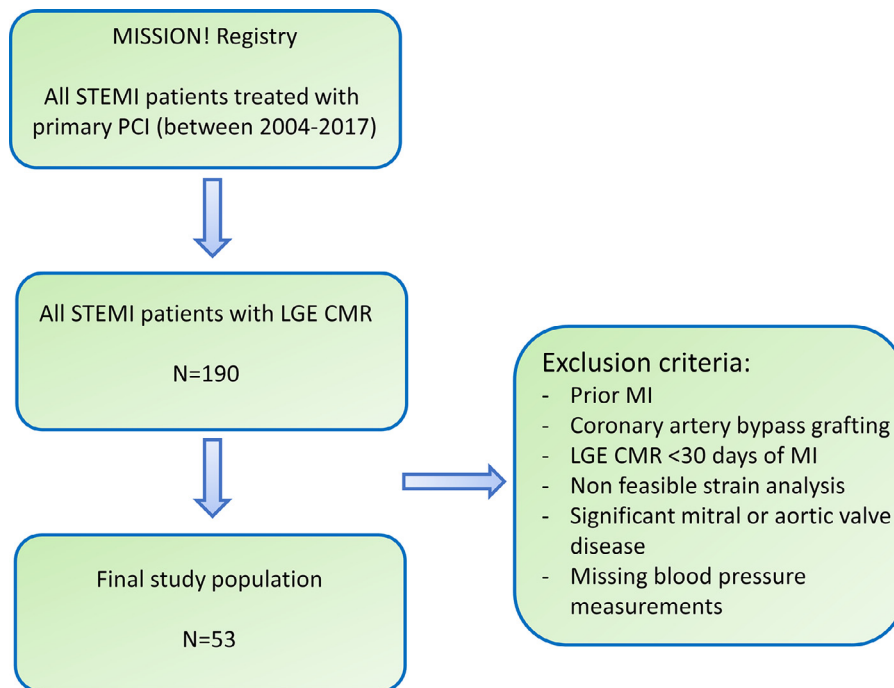


Figure 1. Flow diagram of study population. LGE CMR = late gadolinium enhancement cardiac magnetic resonance; MI = myocardial infarction; PCI = percutaneous coronary intervention; STEMI = ST-segment elevation myocardial infarction.

multivessel disease was defined as the presence of >50% luminal stenosis in more than 1 vessel. Transthoracic echocardiography was performed according to the institutional, guideline-based, clinical care track protocol (MISSION!),<sup>10</sup> while CMR was performed at the discretion of the treating physician. Demographic and clinical data were collected from the departmental cardiology information system (EPD-vision; LUMC, Leiden, The Netherlands) and from electronic medical records (HiX; ChipSoft, Amsterdam, The Netherlands). For retrospective analysis of clinically acquired data, the institutional review board waived the need for individual patient written informed consent.

Using commercially available echocardiographic systems (E9 and E95, General Electric Vingmed Ultrasound, Milwaukee, Wisconsin) transthoracic echocardiographic images were recorded in patients at rest. Electrocardiogram-triggered echocardiographic data were acquired with M5S transducers and digitally stored in cine-loop format for offline analysis (EchoPac 202, General Electric Vingmed Ultrasound). Echocardiographic images from the study closest in time to CMR acquisition were used for analysis. The median interval between echocardiographic and CMR acquisition was 1 month (interquartile range (IQR) 0 to 2 months) and the median interval between STEMI and CMR acquisition was 2 months (IQR 1 to 3 months). LV end-systolic and end-diastolic volumes were measured in apical 2- and 4-chamber views and LV ejection fraction (LVEF) was calculated using the biplane Simpson's method.<sup>11</sup>

Quantification of non-invasive myocardial work was performed using a commercially available software package (EchoPac 202, General Electric Vingmed Ultrasound). Calculation and validation of LV myocardial work analysis from non-invasive LV pressure-strain

loops has been described previously.<sup>8,9</sup> Non-invasive myocardial work was derived from LV pressure-strain loops by integrating LV strain data and non-invasively estimated LV pressure. This approach to echocardiographic quantification of LV work has shown a high degree of correlation with invasively-measured LV myocardial work<sup>8,9,12</sup> and has been validated in several patient subgroups.<sup>8,9,12-15</sup> LV strain data were acquired using 2-dimensional speckle-tracking echocardiography by manually tracing the LV endo- and epicardial borders in the apical long-axis, 2- and 4-chamber views. The automatically generated region of interest was manually adjusted to the myocardial thickness, as required. The LV pressure was assumed to be equal to the arterial blood pressure measured from sphygmomanometric brachial artery cuff measurements. An LV pressure-strain curve was then constructed using a normalized reference curve provided by the software and adjusted to the different cardiac cycle phases using valvular event timing (mitral and aortic valve opening and closing). Strain rate was multiplied with LV pressure and integrated over time to produce segmental and global LV myocardial work.<sup>9,16</sup> Several global and segmental myocardial work indices can be derived from the construction of non-invasive LV pressure-strain loops: myocardial work index (MWI), constructive work (CW), wasted work (WW) and myocardial work efficiency (MWE). MWI is defined as the total LV work performed in a single cardiac cycle. CW is LV myocardial work performed during shortening of a myocardial segment in systole or during lengthening in isovolumic relaxation, thereby contributing to LV ejection. WW on the other hand, is LV myocardial work performed during lengthening of a myocardial segment in systole or during shortening in

isovolumic relaxation, and which therefore does not contribute to LV ejection. MWE is defined as the ratio of CW, divided by the sum of CW and WW, expressed as a percentage.

Patients were imaged on a 1.5-T Gyroscan ACS-NT/Intera MR system (Philips Medical Systems, Best, the Netherlands) or on a 3.0-T Ingenia MR system (Philips Medical Systems, Best, the Netherlands) using retrospective ECG gating. Cine steady-state free precession (SSFP) CMR images were acquired in the long-(2- and 4-chamber views) and short-axes of the LV. Typical imaging parameters were as follows for the 1.5-T Gyroscan ACS-NT/Intera MR system: field of view (FOV)  $400 \times 320$  mm<sup>2</sup>; matrix,  $256 \times 206$  pixels; slice thickness, 10 mm with no slice gap; flip angle ( $\alpha$ ), 35°; echo time (TE), 1.67 ms; and repetition time (TR), 3.3 ms.<sup>17</sup> For the 3.0-T Ingenia MR system typical parameters were: FOV  $400 \times 350$  mm; matrix,  $232 \times 192$  pixels; slice thickness, 8 mm with no slice gap;  $\alpha$ , 45°; TE, 1.5 ms and TR, 3.0 ms.<sup>18</sup> LGE images were acquired 15 minutes after a bolus injection of gadolinium diethylenetriamine pentaacetic acid (Magnevist, Schering, Berlin, Germany) or gadoterate meglumine (Dotarem, Guerbet, Villepinte, France) (0.15 mmol/kg) with an inversion-recovery 3-dimensional turbo-field echo sequence with parallel imaging. The heart was imaged in 1 or 2 breath-holds with short-axis slices at various levels dependent on the heart size. For the 1.5-T Gyroscan ACS-NT/Intera MR system, typical parameters were as follows: FOV  $400 \times 400$  mm<sup>2</sup>; matrix,  $256 \times 206$  pixels; slice thickness, 10 mm with 50% overlap;  $\alpha$ , 10°; TE, 1.06 ms and TR, 3.7 ms.<sup>17</sup> For the 3.0-T Ingenia MR system typical parameters were as follows: FOV  $350 \times 350$  mm; matrix size  $188 \times 125$  mm; acquired pixel size  $1.86 \times 2.8$  mm; reconstructed pixel size  $1.46 \times 1.46$  mm; slice thickness 10 mm with 50% overlap;  $\alpha$ , 10°; SENSE factor 3; TE, 2.09 ms and TR, 4.31 ms.<sup>19</sup> Images were stored digitally for offline analysis.

CMR data analysis was performed with dedicated software (MASS, Leiden University Medical Center, Leiden, the Netherlands). LV endocardial and epicardial borders were manually traced on short-axis SSFP cine images. Myocardial scar was assessed by using a previously reported method, based on the signal intensity (SI).<sup>17</sup> The myocardial segment with the most dense scar was visually identified and a region of interest was placed in this segment to determine the maximum SI. Subsequently, any myocardium with a SI  $\geq 35\%$  of the maximum SI was defined as scar and automatically identified by the software.<sup>17</sup>

The LV was divided into a 13-segment model and each segment was scored based on the percentage of hyperenhancement of the LV myocardial wall: transmural infarcted segments ( $\geq 50\%$ ), non-transmural infarcted segments (1% to 50%) and non-infarcted segments ( $\leq 1\%$ ) (Figure 2). Thereafter, 2 specific regions of interest were defined in the LV myocardial wall according to the percentage of hyperenhancement: the core zone was defined as the segment with the largest extent of transmural hyperenhancement and the remote zone as the myocardial tissue opposite to the core zone, without any evidence of hyperenhancement (Figure 2). If there was evidence of any hyperenhancement in the segment diametrically opposing the core zone, the

first adjacent segment without evidence of hyperenhancement was used as the remote zone. Defining these 2 regions of interest allowed meaningful comparison of echocardiography and CMR LGE data in STEMI patients (Figure 3).

Normally distributed continuous variables are presented as mean  $\pm$  standard deviation (SD) and non-normal continuous variables as median and interquartile range (IQR). Normality was assessed using the Shapiro-Wilk test and visual assessment of a histogram and Q-Q plots. Categorical variables are presented as frequencies and percentages. Continuous variables were compared using the Student's *t*-test if normally distributed and the Mann-Whitney *U*-test if not normally distributed. For comparison of related transmural, non-transmural and non-infarcted segments, linear mixed models were used for normally distributed variables (MWI and CW) and the Friedman's two-way ANOVA with post-hoc Wilcoxon signed-rank tests for non-normally distributed variables (WW and MWE). A *p*-value  $< 0.05$  was considered statistically significant. Statistical analyses were performed using SPSS version 25.0 (SPSS, Armonk, NY).

## Results

Fifty three patients (89% male, age  $58 \pm 9$  years) were analyzed for the presence and distribution of segmental LGE. Patient clinical characteristics are shown in Table 1. Patients received appropriate, guideline-directed pharmacotherapy following STEMI.

Conventional imaging variables, myocardial work indices and LGE burden on CMR are shown in Table 2. The median LVEF was 50% (IQR 44 to 55) and the median global LV MWE 93% (IQR 91 to 96). The mean scar burden was  $14.0 \pm 7.0\%$  of the total LV mass.

All segments ( $n = 689$ ) could be analyzed for LGE and for myocardial work variables. A total of 76 segments (11%) demonstrated transmural hyperenhancement, 280 (41%) had non-transmural hyperenhancement and 333 (48%) segments showed no evidence for hyperenhancement on LGE CMR. An inverse relationship was observed between segmental MWI, CW and MWE and the extent of hyperenhancement transmural on LGE CMR ( $p < 0.05$  for all comparisons) while a trend was observed between a greater amount of WW and transmural hyperenhancement ( $p = 0.086$ ) (Figure 4).

LV myocardial work indices of the infarct core and the remote zone are shown in Figure 5. Segmental MWI, CW and MWE were lower in the core zone (and WW was higher) compared to the remote zone ( $p < 0.05$  for all comparisons).

## Discussion

The findings from our study can be summarized as follows: MWI, CW and MWE decreased significantly with increasing transmural myocardial hyperenhancement, whereas WW increased. Moreover, MWI, CW and MWE were significantly more impaired and WW significantly larger in the core zone compared to the remote zone.

LV myocardial work, the product of force and distance, can be quantified using myocardial force-dimension loops and reflects myocardial oxygen consumption.<sup>20,21</sup> Invasive

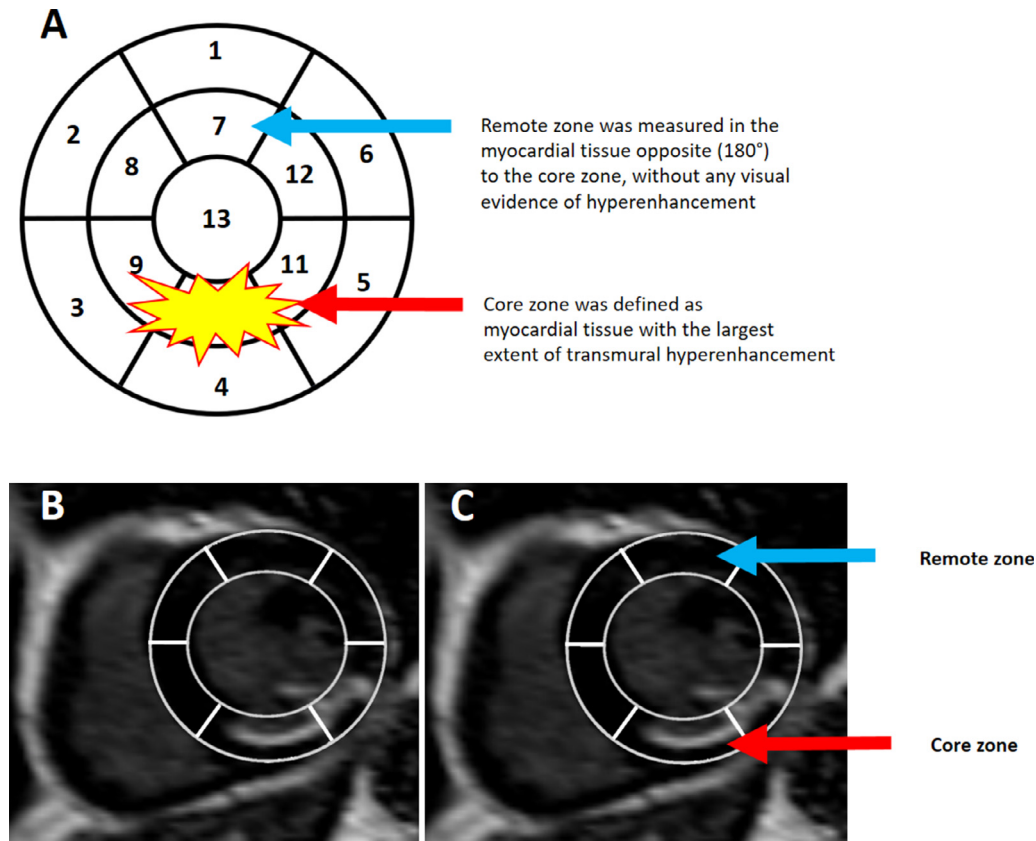


Figure 2. Determining the infarct core and the remote area. The 13-segment model shown in panel A schematically illustrates how the core zone and the remote zone were defined. After the left ventricular (LV) endo- and epicardial borders were traced, the LV segment with most transmural hyperenhancement was defined as the core zone, while the diametrically opposed segment (or next adjacent segment if the segment opposite to the core zone had any evidence of scar), without evidence of hyperenhancement, was labelled as the remote zone. Panels B and C show a patient with late gadolinium enhancement (LGE) on cardiac magnetic resonance (CMR) in the inferior and inferolateral wall after an ST-segment elevation myocardial infarction (STEMI) with complete occlusion of the right coronary artery. The midventricular inferior segment demonstrates an infarct with 73% transmural.

pressure-volume loops have typically been used to measure myocardial work, however, the invasive nature limits its application to daily practice.<sup>21</sup> Russell et al. introduced a non-invasive method to measure myocardial work by incorporating sphygmomanometric brachial artery cuff measurements and echocardiographic speckle tracking strain to construct pressure-strain loops.<sup>8</sup> This novel method demonstrated excellent agreement with invasively measured myocardial work in a canine model under different hemodynamic conditions, as well as in patients with chronic heart failure.<sup>8,9</sup> A robust correlation between non-invasive and invasively measured myocardial work was also found in a study of CRT recipients under different hemodynamic conditions and a variety of CRT settings, e.g. CRT off, LV pacing only, right ventricular pacing only, standard biventricular pacing and multipoint biventricular pacing.<sup>12</sup> Regional non-invasive myocardial work corresponds to regional glucose metabolism measured with <sup>18</sup>F-fluorodeoxyglucose (<sup>18</sup>F-FDG) positron emission tomography (PET), confirming its validity as a measure of myocardial energetics.<sup>8</sup>

While LVEF and global LV longitudinal strain remain pillars of LV function assessment, they are limited by load-dependency.<sup>22</sup> Skulstad et al. demonstrated that the contraction of ischemic myocardium is heavily dependent on

afterload.<sup>23</sup> Non-invasive myocardial work assessment has the ability to integrate the LV contraction and afterload into a single parameter, which represents a more comprehensive index of LV performance than either contractile function or afterload in isolation. Boe et al. found non-invasive myocardial work to be superior to strain analysis for the identification of acute coronary vessel occlusion in patients with non-STEMI.<sup>13</sup> In ischemic but viable myocardial segments, metabolism is reduced and can be quantified with <sup>18</sup>F-FDG PET.<sup>24</sup> The firm correlation between regional non-invasive myocardial work and regional glucose metabolism raises the exciting possibility that non-invasive myocardial work indices may reflect segmental energetics, and allow the identification of myocardial viability.<sup>8</sup> LGE CMR is a proven indicator of myocardial viability through accurate distinction between viable myocardium and of nonviable scar.<sup>5</sup> LGE CMR is a reliable predictor of myocardial functional recovery following revascularization. In a population of 50 patients with ischemic ventricular dysfunction, Kim et al. demonstrated segmental recovery in 8% of segments with transmural hyperenhancement compared to 66% in non-transmural hyperenhancement.<sup>1</sup> The inverse relation between the transmural extent of LGE on CMR and segmental recovery following revascularization has been demonstrated in numerous studies.<sup>25</sup> The significant inverse



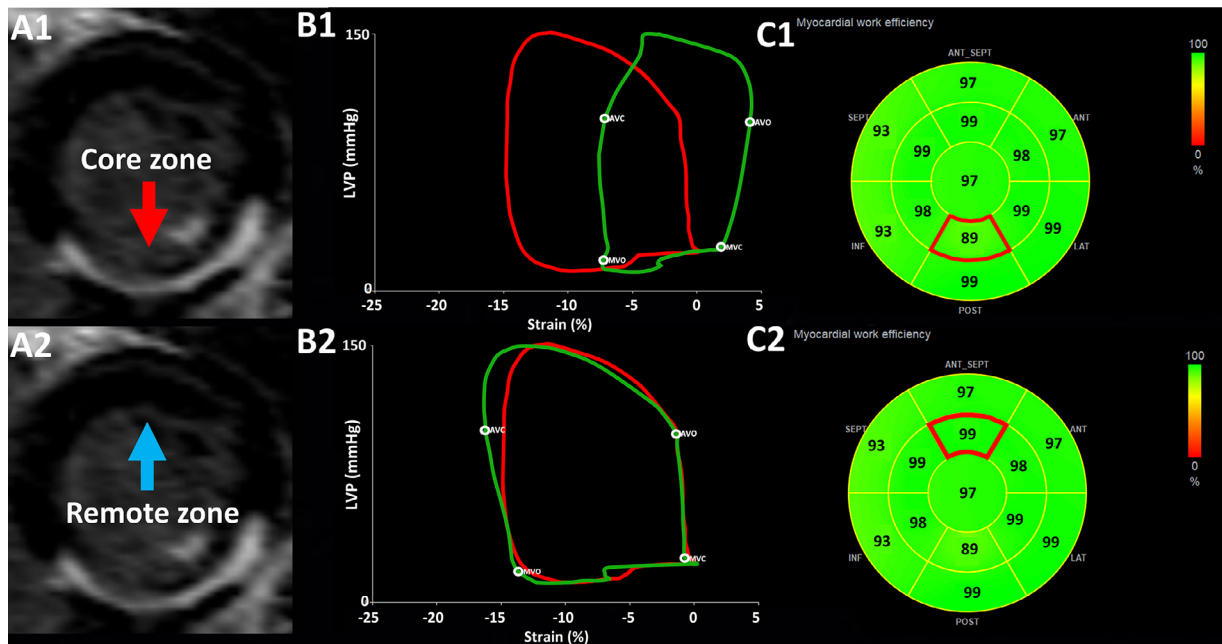


Figure 3. Non-invasive pressure-strain loops and myocardial work efficiency of a patient after an ST-segment elevation myocardial infarction (STEMI). A 41 year old male patient presented with an inferior STEMI, due to complete occlusion of the right coronary artery. On late gadolinium contrast enhanced cardiac magnetic resonance (LGE CMR) imaging the total scar burden was 11.9%. Panel A represents the core zone with 73% transmural (A1) and the remote zone (A2) on LGE CMR. Panel B displays non-invasive pressure-strain loops from which myocardial work efficiency is derived (B1 core zone and B2 remote zone). The red pressure-strain loop represents the averaged loop for all left ventricular segments, whereas the green pressure-strain loop specifically represents the selected segment outlined in Panel C. Panel C shows parametric maps of left ventricular myocardial work efficiency (C1 core zone with myocardial work efficiency (MWE) of 89% and C2 remote zone MWE of 99%).

Table 1  
Patient characteristics

Variable	(n = 53)
Age (years)	58 ± 9
Men	47 (89%)
Height (cm)	178.4 ± 6.7
Weight (kg)	87.6 ± 14.0
BMI (kg/m <sup>2</sup> )	27.5 ± 4.1
BSA (m <sup>2</sup> )	2.1 ± 0.2
LAD culprit artery	33 (62%)
Peak creatine phosphokinase (U/L)	2665 (1397-4661)
Peak troponin T (μg/L)	6.8 (4.0-11.3)
Creatinine (μmol/L)	81 (71-89)
Hypertension	24 (45%)
Hypercholesterolemia	13 (25%)
Diabetes mellitus	6 (11%)
Current smoker	26 (49%)
Family history of CVD	21 (40%)
<i>Medication at discharge</i>	
Aspirin	51 (96%)
Thienopyridine	53 (100%)
β-blocker	52 (98%)
Statin	53 (100%)
ACE-I/ARB	53 (100%)

Values are mean ± standard deviation if normally distributed and median (interquartile range) if not normally distributed.

ACE-I: angiotensin-converting enzyme inhibitor, ARB: angiotensin receptor blocker, BMI: body mass index, BSA: body surface area, CV: cardiovascular, CVD: cardiovascular disease, LAD: left anterior descending coronary artery.

relationship between segmental CW and transmural hyper-enhancement on LGE CMR is a new insight this study provides and might indicate CW to be a valid measure of viability of myocardial segments.

Following STEMI, an inflammatory response may occur in the remote zone, eventually leading to interstitial fibrosis.<sup>2,3,26</sup> Several studies have investigated changes in contractile function of the remote zone following a myocardial infarction, and while some reported preserved systolic function,<sup>27</sup> others demonstrated reduced function.<sup>2</sup> In a

Table 2  
Imaging variables

Variable	(n = 53)
<i>Conventional echocardiographic variables</i>	
Left ventricular end-diastolic volume (ml)	113 (89-142)
Left ventricular end-systolic volume (ml)	58 (42-84)
Left ventricular ejection fraction (%)	50 (44-55)
<i>Myocardial work indices</i>	
Global myocardial work index (mmHg%)	1446 ± 412
Global constructive work (mmHg%)	1671 ± 474
Global wasted work (mmHg%)	77 (58-127)
Global left ventricular (LV) myocardial work efficiency (%)	93 (91-96)
<i>LGE CMR</i>	
Total LV mass (g)	162 ± 41
Total scar burden (%)	14.0 ± 7.0

Values are mean ± standard deviation if normally distributed and median (interquartile range) if not normally distributed.

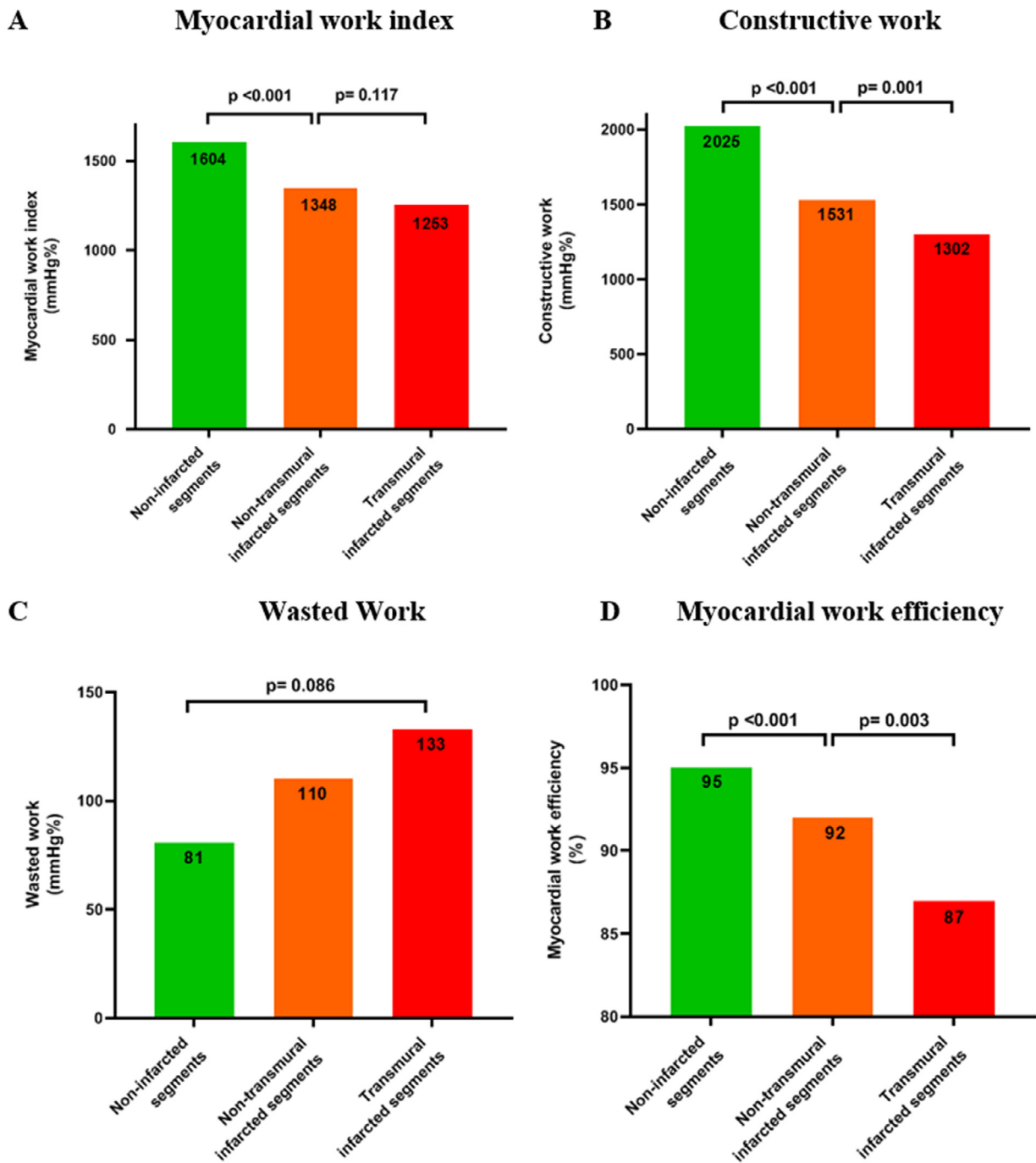


Figure 4. Myocardial work indices stratified according to infarct transmurality on late gadolinium enhancement cardiac magnetic resonance (LGE CMR). The segmental values of different myocardial work indices are presented, according to infarct transmurality on LGE CMR. Segmental values for myocardial work index (A), constructive work (B) and myocardial work efficiency (D) according to transmurality on LGE CMR.

murine model of myocardial infarction, Espe et al. demonstrated that a redistribution of myocardial work occurred from the infarcted segments to the remote zone.<sup>28</sup> Our data also indicate preserved or enhanced remote zone myocardial work, compared to the infarct core. The remote zone is an emerging region of interest for post-infarct risk-stratification. In a population of 288 reperfused STEMI patients who underwent CMR, native T1 values of the remote zone on CMR were independently associated with LV remodeling at 6 months, as well as with major adverse cardiac

events.<sup>3</sup> Similar results were found in a study by Reinstandler and co-workers of 255 STEMI patients, where native T1 values of the remote zone provided incremental prognostic information beyond established markers of infarct severity.<sup>4</sup> Myocardial work has been compared between the remote and core zones of an infarct in a murine model.<sup>29</sup> In non-failing LVs, myocardial work was increased in the remote zone when compared to controls. In contrast, a compensatory increase in myocardial work in the remote zone was not seen in rats who developed cardiac failure.<sup>29</sup>

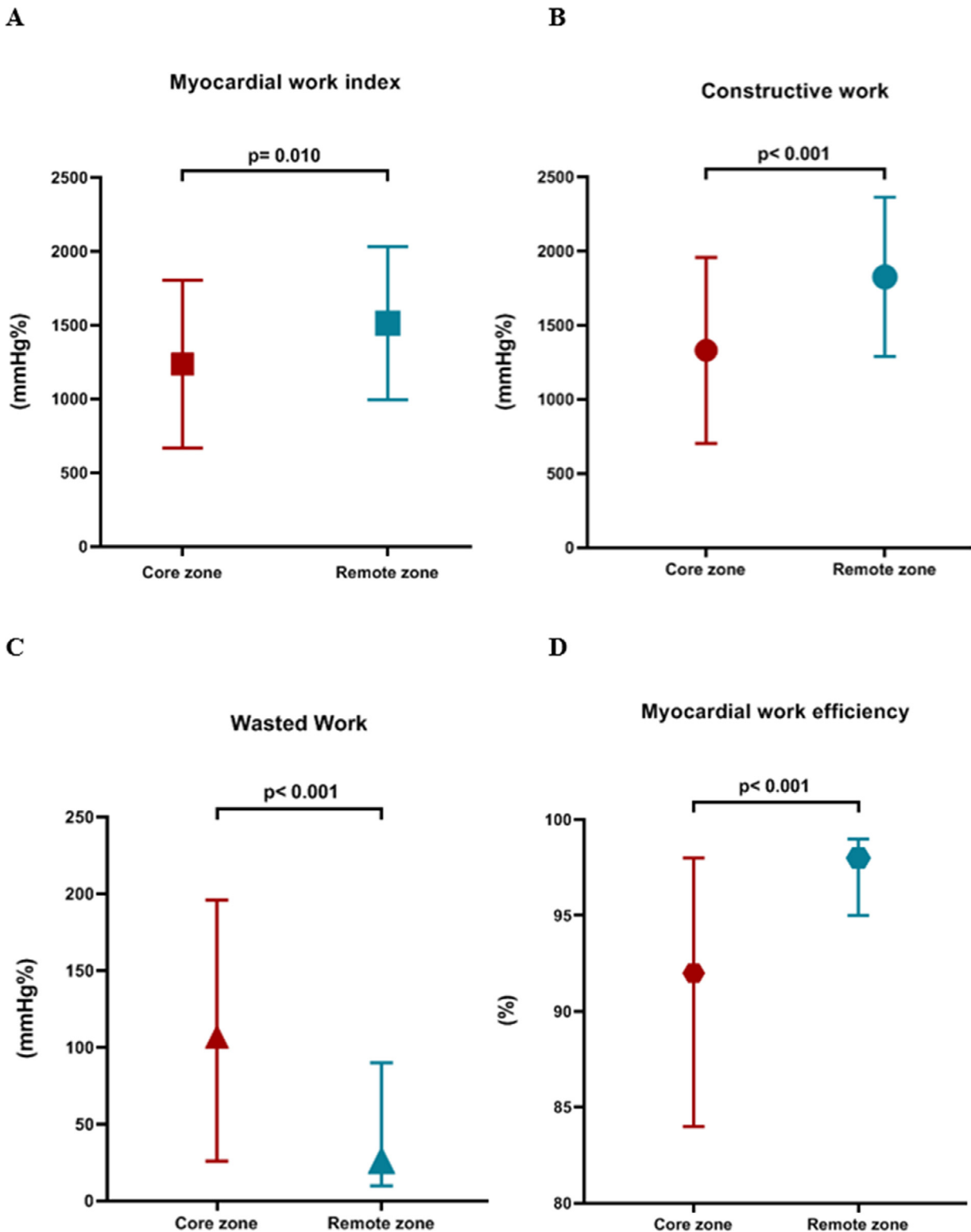


Figure 5. Myocardial work indices in core and remote infarct zones. The values presented in the box-and-whisker plot for panels (A) and (B) are mean  $\pm$  standard deviation and median (interquartile range) for panels (C) and (D).

Several limitations should be acknowledged. This was a single center study with a retrospective design. Patients in whom echocardiographic speckle tracking strain analysis could not be performed had to be excluded. Patients with significant aortic stenosis or patients with missing blood

pressure measurements were excluded and this may have led to a selection bias. The remote zone was defined as the non-infarcted myocardial segment diametrically opposed to the infarct core, and was adopted as a reference for normal, non-invasive myocardial work values. Although

such LV segments were distant from the infarct, abnormal T1 values have been recognized in the remote zone. While the significance of this finding is still unclear, it suggests that the remote zone does not represent altogether normal myocardium.<sup>2-4</sup> We included a homogeneous population, the value of non-invasive myocardial work in a heterogeneous population should be investigated. The findings of our study should be confirmed in larger, multi-center studies before implementation in clinical practice.

In conclusion, in post-STEMI patients that underwent primary PCI, CW and MWE were significantly lower in the transmural infarcted segments and non-invasive myocardial work parameters significantly different in the remote and core zone. Segmental CW may therefore serve as a low cost, non-invasive marker of myocardial viability. Furthermore, we demonstrated that non-invasive myocardial work can be utilized for the characterization of the remote, which is an emerging prognostic marker and therapeutic target post-STEMI.

### Credit author statement

*Mohammed El Mahdiui*: Conceptualization; Data curation; Formal analysis; Investigation; Methodology; Project administration; Resources; Validation; Visualization; Writing - original draft. *Pieter van der Bijl*: Conceptualization; Data curation; Methodology; Resources; Validation; Writing - review & editing. *Rachid Abou*: Conceptualization; Data curation; Methodology; Resources; Validation; Writing - review & editing. *Rodolfo de Paula Lustosa*: Conceptualization; Data curation; Methodology; Resources; Validation; Writing - review & editing. *Rob van der Geest*: Data curation; Resources; Validation; Writing - review & editing. *Nina Ajmone Marsan*: Conceptualization; Funding acquisition; Methodology; Project administration; Supervision; Validation; Writing - review & editing. *Victoria Delgado*: Conceptualization; Data curation; Funding acquisition; Methodology; Project administration; Resources; Supervision; Validation; Writing - review & editing. *Jeroen J. Bax*: Conceptualization; Data curation; Funding acquisition; Methodology; Project administration; Resources; Supervision; Validation; Writing - review & editing.

### Conflict of interest

The authors declare that they have no known competing financial interests or personal relationships that could have appeared to influence the work reported in this paper.

### Disclosures

Rodolfo P. Lustosa received funding from the European Society of Cardiology in form of ESC Research Grant (R-2018-17759). We declare the following conflict of interests: the department of Cardiology received unrestricted research grants from Abbott Vascular, Bayer, Bioventrix, Biotronik, Boston Scientific, Edwards Lifesciences, GE Healthcare and Medtronic. Victoria Delgado received speaker fees from Abbott Vascular, Edwards Lifesciences, GE Healthcare and Medtronic. Nina Ajmone Marsan and Jeroen J Bax

received speaker fees from Abbott Vascular. The remaining authors have nothing to disclose.

- Kim RJ, Wu E, Rafael A, Chen E-L, Parker MA, Simonetti O, Klocke FJ, Bonow RO, Judd RM. The use of contrast-enhanced magnetic resonance imaging to identify reversible myocardial dysfunction. *N Engl J Med* 2000;343:1445-1453.
- Chan W, Duffy SJ, White DA, Gao XM, Du XJ, Ellims AH, Dart AM, Taylor AJ. Acute left ventricular remodeling following myocardial infarction: coupling of regional healing with remote extracellular matrix expansion. *JACC Cardiovasc Imaging* 2012;5:884-893.
- Carrick D, Haig C, Rauhalammi S, Ahmed N, Mordi I, McEntegart M, Petrie MC, Eteiba H, Lindsay M, Watkins S, Hood S, Davie A, Mahrous A, Sattar N, Welsh P, Tzemos N, Radjenovic A, Ford I, Oldroyd KG, Berry C. Pathophysiology of LV remodeling in survivors of STEMI: inflammation, remote myocardium, and prognosis. *JACC Cardiovasc Imaging* 2015;8:779-789.
- Reinstadler SJ, Stiermaier T, Liebetrau J, Fuernau G, Eitel C, de Waha S, Desch S, Reil JC, Poss J, Metzler B, Lucke C, Gutberlet M, Schuler G, Thiele H, Eitel I. Prognostic significance of remote myocardium alterations assessed by quantitative noncontrast T1 mapping in ST-segment elevation myocardial infarction. *JACC Cardiovasc Imaging* 2018;11:411-419.
- Kim RJ, Fieno DS, Parrish TB, Harris K, Chen EL, Simonetti O, Bundy J, Finn JP, Klocke FJ, Judd RM. Relationship of MRI delayed contrast enhancement to irreversible injury, infarct age, and contractile function. *Circulation* 1999;100:1992-2002.
- Mahrholdt H, Wagner A, Holly TA, Elliott MD, Bonow RO, Kim RJ, Judd RM. Reproducibility of chronic infarct size measurement by contrast-enhanced magnetic resonance imaging. *Circulation* 2002;106:2322-2327.
- Eitel I, de Waha S, Wöhrle J, Fuernau G, Lurz P, Pauschinger M, Desch S, Schuler G, Thiele H. Comprehensive prognosis assessment by CMR imaging after ST-segment elevation myocardial infarction. *JACC* 2014;64:1217-1226.
- Russell K, Eriksen M, Aaberge L, Wilhelmsen N, Skulstad H, Remme EW, Haugaa KH, Opdahl A, Fjeld JG, Gjesdal O, Edvardsen T, Smiseth OA. A novel clinical method for quantification of regional left ventricular pressure-strain loop area: a non-invasive index of myocardial work. *Eur Heart J* 2012;33:724-733.
- Russell K, Eriksen M, Aaberge L, Wilhelmsen N, Skulstad H, Gjesdal O, Edvardsen T, Smiseth OA. Assessment of wasted myocardial work: a novel method to quantify energy loss due to uncoordinated left ventricular contractions. *Am J Physiol Heart Circ Physiol* 2013;305:H996-1003.
- Liem SS, van der Hoeven BL, Oemrawsingh PV, Bax JJ, van der Bom JG, Bosch J, Viergever EP, van Rees C, Padmos I, Sedney MI, van Exel HJ, Verwey HF, Atsma DE, van der Velde ET, Jukema JW, van der Wall EE, Schalij MJ. MISSION!: optimization of acute and chronic care for patients with acute myocardial infarction. *Am Heart J* 2007;153. 14.e11-11.
- Lang RM, Badano LP, Mor-Avi V, Filalo J, Armstrong A, Ernande L, Flachskampf FA, Foster E, Goldstein SA, Kuznetsova T, Lancellotti P, Muraru D, Picard MH, Rietzschel ER, Rudski L, Spencer KT, Tsang W, Voigt JU. Recommendations for cardiac chamber quantification by echocardiography in adults: an update from the American Society of Echocardiography and the European Association of Cardiovascular Imaging. *Eur Heart J Cardiovasc Imaging* 2015;16:233-270.
- Hubert A, Le Rolle V, Leclercq C, Galli E, Samset E, Casset C, Mabo P, Hernandez A, Donal E. Estimation of myocardial work from pressure-strain loops analysis: an experimental evaluation. *Eur Heart J Cardiovasc Imaging* 2018;19:1372-1379.
- Boe E, Russell K, Eek C, Eriksen M, Remme EW, Smiseth OA, Skulstad H. Non-invasive myocardial work index identifies acute coronary occlusion in patients with non-ST-segment elevation-acute coronary syndrome. *Eur Heart J Cardiovasc Imaging* 2015;16:1247-1255.
- El Mahdiui M, van der Bijl P, Abou R, Ajmone Marsan N, Delgado V, Bax JJ. Global left ventricular myocardial work efficiency in healthy individuals and patients with cardiovascular disease. *J Am Soc Echocardiogr* 2019;32:1120-1127.
- Manganaro R, Marchetta S, Dulgheru R, Ilardi F, Sugimoto T, Robinet S, Cimino S, Go YY, Bernard A, Kacharava G, Athanassopoulos GD, Barone D, Baroni M, Cardim N, Hagedorff A, Hristova K, Lopez-Fernandez T, de la Morena G, Popescu BA, Penicka M, Ozyigit T,



- Rodrigo Carbonero JD, van de Veire N, Von Bardeleben RS, Vineranu D, Zamorano JL, Rosca M, Calin A, Moonen M, Magne J, Cosyns B, Galli E, Donal E, Carerj S, Zito C, Santoro C, Galderisi M, Badano LP, Lang RM, Oury C, Lancellotti P. Echocardiographic reference ranges for normal non-invasive myocardial work indices: results from the EACVI NORRE study. *Eur Heart J Cardiovasc Imaging* 2019;20:582–590.
16. van der Bijl P, Kostyukevich M, El Mahdiui M, Hansen G, Samset E, Ajmone Marsan N, Bax JJ, Delgado V. A roadmap to assess myocardial work: from theory to clinical practice. *JACC Cardiovasc Imaging* 2019;12:2549–2554.
17. Roes SD, Borleffs CJ, van der Geest RJ, Westenberg JJ, Marsan NA, Kaandorp TA, Reiber JH, Zeppenfeld K, Lamb HJ, de Roos A, Schalij MJ, Bax JJ. Infarct tissue heterogeneity assessed with contrast-enhanced MRI predicts spontaneous ventricular arrhythmia in patients with ischemic cardiomyopathy and implantable cardioverter-defibrillator. *Circ Cardiovasc Imaging* 2009;2:183–190.
18. Tao Q, van der Tol P, Berendsen FF, Paiman EHM, Lamb HJ, van der Geest RJ. Robust motion correction for myocardial T1 and extracellular volume mapping by principle component analysis-based groupwise image registration. *J Magn Reson Imaging* 2018;47:1397–1405.
19. Bizino MB, Tao Q, Amersfoort J, Siebelink HJ, van den Bogaard PJ, van der Geest RJ, Lamb HJ. High spatial resolution free-breathing 3D late gadolinium enhancement cardiac magnetic resonance imaging in ischaemic and non-ischaemic cardiomyopathy: quantitative assessment of scar mass and image quality. *Eur Radiol* 2018;28:4027–4035.
20. Hisano R, Cooper Gt. Correlation of force-length area with oxygen consumption in ferret papillary muscle. *Circ Res* 1987;61:318–328.
21. Delhaas T, Arts T, Prinzen FW, Reneman RS. Regional fibre stress-fibre strain area as an estimate of regional blood flow and oxygen demand in the canine heart. *J Physiol* 1994;477(Pt 3):481–496.
22. Yingchoncharoen T, Agarwal S, Popovic ZB, Marwick TH. Normal ranges of left ventricular strain: a meta-analysis. *J Am Soc Echocardiogr* 2013;26:185–191.
23. Skulstad H, Edvardsen T, Urheim S, Rabben SI, Stugaard M, Lyseggen E, Ihlen H, Smiseth OA. Postsystolic shortening in ischemic myocardium: active contraction or passive recoil? *Circulation* 2002;106:718–724.
24. Elsasser A, Muller KD, Skwara W, Bode C, Kubler W, Vogt AM. Severe energy deprivation of human hibernating myocardium as possible common pathomechanism of contractile dysfunction, structural degeneration and cell death. *JACC* 2002;39:1189–1198.
25. Romero J, Xue X, Gonzalez W, Garcia MJ. CMR imaging assessing viability in patients with chronic ventricular dysfunction due to coronary artery disease: a meta-analysis of prospective trials. *JACC Cardiovasc Imaging* 2012;5:494–508.
26. Ugander M, Oki AJ, Hsu LY, Kellman P, Greiser A, Aletras AH, Sibley CT, Chen MY, Bandettini WP, Arai AE. Extracellular volume imaging by magnetic resonance imaging provides insights into overt and sub-clinical myocardial pathology. *Eur Heart J* 2012;33:1268–1278.
27. Husser O, Chaustre F, Sanchis J, Nunez J, Monmeneu JV, Lopez-Lereu MP, Bonanad C, Gomez C, Oltra R, Llacer A, Riegger GA, Chorro FJ, Bodi V. Function of remote non-infarcted myocardium after STEMI: analysis with cardiovascular magnetic resonance. *Int J Cardiovasc Imaging* 2012;28:2057–2064.
28. Espe EK, Aronsen JM, Eriksen GS, Zhang L, Smiseth OA, Edvardsen T, Sjaastad I, Eriksen M. Assessment of regional myocardial work in rats. *Circ Cardiovasc Imaging* 2015;8:e002695.
29. Espe EK, Aronsen JM, Eriksen M, Sejersted OM, Zhang L, Sjaastad I. Regional dysfunction after myocardial infarction in rats. *Circ Cardiovasc Imaging* 2017;10(9):e005997. <https://doi.org/10.1161/CIRCIMAGING.116.005997>.